

FRACTURE TOUGHNESS OF FERRITIC STEEL - UNDERWATER WET WELDED

Roberto Francisco Di Lorenzo *

*CDTN – Nuclear Technology Development Center
CNEN – Brazilian National Nuclear Energy Commission
Campus UFMG - Belo Horizonte – MG - Brazil – 30.123-970
Phone: +55-31-34993165 Fax:+55-31-34993390
E-mail: rfl@cdtn.br*

Wellington Antonio Soares
*CDTN – Nuclear Technology
Development Center
CNEN – Brazilian National Nuclear
Energy Commission*

Alexandre Queiroz Bracarense
*Mechanical Engineering Department
UFMG – Federal University of Minas
Gerais*

ABSTRACT

Life extension of structures, such as nuclear power plants or nuclear reactor internals could require recoveries or mitigation actions due to aging phenomena. Such actions on steel structures many times has to be done using welds in wet environment, what would require special techniques like underwater wet welding.

Shielded metal-arc welding is usually used in underwater wet welding. Once the welding electric arc is open, water dissociation occurs, producing oxygen, hydrogen, and characteristic welding gases. These produced chemical elements can be absorbed by the weld in underwater wet welding process and due to the fast cooling of weld it is impossible to eliminate these welding gases. Higher levels of absorbed discontinuities are characteristics of underwater wet welding. Cooling rate of underwater wet welding is faster than conventional air welding. Structures built using underwater wet welding must attend to special structural requirements.

Results of fracture toughness of materials produced with high cooling rate and high level of inherent discontinuities, characteristic of underwater wet welding process, are presented in this paper. Materials used in this work were welded in depth condition of 0, 20, 40 and 60 meters of water column.

Keywords: Fracture Toughness, Underwater Wet Welding, Life Management, Master Curve, Reference Temperature.

1. INTRODUCTION

Aging of nuclear power plants or nuclear reactor internals could require recoveries or mitigation actions to allow life management or life extension of such structures.

Pressure vessels and internals components of nuclear reactors need special cares. Sometimes, these component recoveries could be demanded after being irradiated. Recovery of the internals or of the nuclear reactors components, after the operation had started, could be done using underwater welding. Recoveries of nuclear components are allowed to be done using underwater wet welding or underwater dry welding. Underwater welding is less expensive than drying the component, taking it out, welding and then returning it to its original

place. Underwater welding allows moderation of irradiation on technician doing such tasks and resulting in less overall individual dose.

Underwater wet welding used to recover parts does not present, however, the same quality of the weld recovered in dry environment, which has very established procedures.

Recovering or building components using underwater wet welding create discontinuities that are inherent to the process and are difficult to live together during its in-service or remaining life. These discontinuities, like porosity, non-metallic inclusions, among others, must be measured and known. This knowledge allows checking the agreement of the structure to the standards and effective codes.

Structural integrity evaluation of mechanical systems should be accomplished when underwater welded is used in construction or repair. Such evaluations usually consist in calculations, non-destructive examination, fracture mechanics methods and others appropriate techniques

These techniques of inspections and tests are used, however, to check or to evaluate "perfect materials", or materials without discontinuities. Techniques like fracture mechanics also works with "perfect materials", with specific crack sizes in "perfect materials", without any other discontinuity. Crack propagation with determined size, direction, geometry, position, and deformation rate is considered when working with fracture mechanics.

The reality is other when working with built or recovered structures using underwater wet welding process. The discontinuities in underwater wet welding structure could allow crack propagation once they could not immobilize them, when subjected to such effects. Discontinuities could be or not a crack initiation point. The situation that follows now is how these discontinuities behave. Mechanical behavior of one structure with more discontinuities than in a conventional component is then the subject of this work.

To reach this objective, coupons of ferritic steel with dimensions 300 mm x 150 mm x 16 mm were underwater wet welded, with a Shielded Metal Arc Welding (SMAW), inside a water tank with hydrostatic pressures applied from 0 to 60 meters of water column to obtain samples with characteristic discontinuities of this process.

2. UNDERWATER WET WELDING.

Underwater wet welding is performed directly inside the water with the SMAW - Shielded Metal Arc Welding Process, without any other physical protection between the water and the arc of welds.

The water in the surrounding atmosphere, during the underwater wet welding, is dissociated by the electric arc in oxygen and hydrogen and it also acts as environment of fast cooling, similar to a quenching, that hardens the welds and the heat affected zone. The hydrogen and the oxygen dissociated can be absorbed by the liquid bath of metal, due to the fast solidification of the welds, and the welded joint becomes susceptible to the hydrogen cracking, resulting in an abnormal amount of pores and absorbed oxygen.

The pores formation is resulted from the absorption and over saturation of dissolved gases or production of gases by chemical reaction. The nature and the amount of pores depend on pore nucleation processes, growth, transport and coalescence of such pores.

The formation of the pores is controlled by the solubility of several gases, mainly the hydrogen, in the melted metal. The solubility of gases is reduced when the material is solidified. During the solidification process, dissolved gases are rejected with the molecules that form the bubbles. In underwater wet welding, the solidification is so fast that prevent the outlet of those bubbles from the surface of the melted bath, and, therefore, they are absorbed in the solidified metal. The pores reduce the resistant area and reduce consequently the resistance, the ductility and the toughness of the structure.

Suga and Hasui (1986) studied the porosities problems in underwater wet welding considering several depths of water. The level of resulting porosities was measured and presented a stable percentile increase in porosity with the increase of depth. The porosity is not formed until a 0.5 atm pressure, increasing up to 9% in welding at 6 atm. It was also observed that there are two morphologies of the produced pores, at lower and at higher pressures. In material welded up to 2 - 3 atm, the pores are formed close to the fusion line and they grow in the direction of the solidification lines and are more spherical. In materials welded between 3 and 6 atm, the pores have the tendency to occur in the superior part of the weld bath. They are more elongated, with porosity in a tubular form. In material welded at intermediate pressures between those two bands, 3 atm, both types of pores are observed together in the weld metal. The morphologies for forming pores are different at high and low pressures.

Standard AWS D 3.6 - 99 specifies the acceptable amount of porosities, size distribution and density in underwater wet welding. Pores with diameters larger than 5 mm are not acceptable. Pores between 1.6 and 5 mm are restricted to the maximum of 0.28 pores/mm (7 pores for inch) in the length of welds for thickness of 25.4 mm (1 inch). Pores with dimensions smaller than 1.6 mm do not have restrictions.

The effects of porosities in the mechanical properties in underwater wet welding are not studied experimentally, according to Danninger et alii (1993). Young's Module, yield and strength limits, ductility and toughness were determined and in general these properties decrease with the increase in the porosity. The toughness and the ductility are more affected than the yield and strength limits (DANNINGER et alii, 1993).

Matlock et alii (1987) determined that the pores are effective anchors of crack fronts, delaying the rate of propagation of these cracks in fatigue with low stress intensity factor. However, if the stress intensity factor is higher, the growth of the crack is accelerated in the presence of porosity.

The underwater wet weld bead has characteristic porosity of this welding process and is acceptable. The effect of that porosity in crack propagation by fatigue should be evaluated.

3. FRACTURE TOUGHNESS

Mechanical properties of welded materials that use underwater wet welding processes are lower than those performed in air welding. AWS D 3.6 - 99 standard specifies the tests that should be accomplished for determining the mechanical properties for each type of weld. Material with wet weld has reduced the strength limit, the elongation, the reduction of area, the bending ductility, Charpy impact testing toughness, in comparison with the same, dry, welded material in dry air. Welding discontinuities, such as slag inclusions, lack of penetration, lack of fusion, cracking, undercutting and porosity, can be enlarged with the increase of the depth of welding (WATSON et alii, 1994).

The treatment of fracture toughness data is used in the analysis of fracture mechanics and depends on the types of available data. This dependence makes difficult the structural integrity evaluation, when applying only a simplified procedure. Data of fracture toughness cannot be available in all situations, or they cannot be easily obtained due to the lack of material or the impossibility of removing material from an actual structure. In these cases, the Charpy impact data can be all the available and reliable correlation between the Charpy impact energy and the fracture toughness should be found.

In the study of fracture toughness of ferritic steels a reference temperature T_0 be determined. The fracture toughness of these ferritic steels can be established starting from cleavage, in the elastic area, or from the elastic-plastic instability, K_{Jc} , or both.

The ferritic steels should have yield limit between 275 and 825 MPa, as well as the weld bead that have resistance different from the base-metal of 10% or smaller (ASTM E 1921 - 02).

The material for studying fracture toughness should be preferentially macroscopically uniform, with tensile and toughness properties without great variations from one area to other. For instance, multi-pass welds can create heat-affected zones and brittle zones with local properties very different from the base material and the weld, what could produce statistical dispersion of the results.

In the study of fracture toughness, is used notched and pre-cracked specimens, with defined crack sizes. Stresses and stress intensity factor K are required, in the temperature range. Cleavage or pop-in development crack during the loading of the specimen can occur.

The J-Integral values in the instability, J_c , are calculated and converted into unit equivalent to the stress-intensity factor K_{Jc} . The tests are repeated, at least six times, can be used to estimate the median $K_{Jc(\text{median})}$. Wide scattering is waited among the results of the repetitions.

Fracture toughness is calculated in defined conditions of crack instability. The crack aspect ratio a/W is equal to 0.5. The width of the bending sample can be one or twice the thickness.

For materials that operate in brittle condition, the determination of fracture toughness starting from the Charpy impact data follows the concept of the Master Curve. This concept is based on the correlation between the temperature of testing, for Charpy impact energy equal to 28 J, and the temperature for $K_{Jc} = 100 \text{ MPa}\cdot\text{m}^{1/2}$. Although originally developed in function of T_{28J} , the approach can be considered applicable to the equivalent temperature corresponding to 28 J, as defined in the specifications of many structural steels (NEVASMMAA et alii, 1998).

The position of the toughness transition curve on the temperature coordinate is established with the experimental determination of the temperature T_0 , in the which one hope to be $K_{Jc(\text{median})}$ for sample of size $1T$ (an inch of thickness) is $100 \text{ MPa}\cdot\text{m}^{1/2}$.

3. METHODOLOGY

Submerged wet welding were executed, using Shielded Metal electrodes AWS E 6013, welded in steel plates ASTM A-36 with 16 and 25 mm of thickness, 300 mm length and 150 mm width. The ASTM A-36 base-material

was inside the specified limits of carbon equivalent, smaller than 0.40%, according to the AWS D 3.6 - 99 Standard.

The material was welded inside a pressure vessel with water, shown in FIG. 3.1, in top in a 40° beveled, with 6 mm of separation between the plates. Shielded metal electrodes were used with 5 mm of diameter and 450 mm of length, dry in oven and covered with varnish protection against humidity absorption.



FIGURE 3.1 – Pressure Vessel manufactured for simulating underwater wet welding up to 100 meters of water column

The pressure vessel was designed, mounted and tested in the Nuclear Technology Development Center - CDTN, from Brazilian National Nuclear Energy Commission - CNEN and in the Laboratory of Robotics, Welding and Simulation - LRSS – from the Mechanical Engineering Department of the Federal University of Minas Gerais - DEMEC/UFMG.

The wet welding was performed in pressures corresponding to zero meter of water column (wcm), 20 wcm, 40 wcm and 60 wcm. The electric arc was opened directly inside the water, without any physical protection among the water, electrode, and the specimen to be welded. The shielded metal electrode deposition in the specimen during the submerged wet welding was automatic, by gravity. While the electrode was consumed, the fixation headstock was moved down.



FIGURE 3.2 – Submerged wet welding inside a tank open electric arc is illustrated. (Note the welding fumes).

These welded coupons were non-destructively inspected and checked against the AWS D3.6-99 Standard.

Charpy type specimens, with dimensions of 10 mm x 10 mm x 55mm, were machined in order to be subjected to impact testing at several temperatures and to toughness fracture measurement. Charpy transition temperatures for different depths of welding were determined. A 27 J equivalent temperature was used for determining the fracture toughness.

Single edge notched bend bars SE(B) were used for determining the fracture toughness of the ferritic steel. The Charpy type SE(B) specimen has a span-to width ratio equal to 4, and crack size $a_0 = 5.0 \text{ mm} \pm 0.5 \text{ mm}$. The fracture toughness temperature was determined considering the results from the impact Charpy test.

4. RESULTS AND DISCUSSION

Charpy instrumented impact tests were accomplished in several welded materials and the Charpy transition curves with the temperatures were determined. The Charpy specimens with 10 mm x 10 mm x 55 mm, of dimension and type V-notched, with 2 mm of depth were cut in the middle of the thickness of the transversal sections of the welds. The V-notched were machined in order to propagate of the fracture in the longitudinal direction of the welds (direction L-T), as shown in FIG 4.1, to evaluate the behavior of the fracture in the bead of the submerged wet welds, in the area of smaller resistance of the material. The bead in the submerged wet welding was the critical area of that structure, and the propagation happened not only to cross the structure in the direction S-L or L-S, but longitudinally to the weld bead.

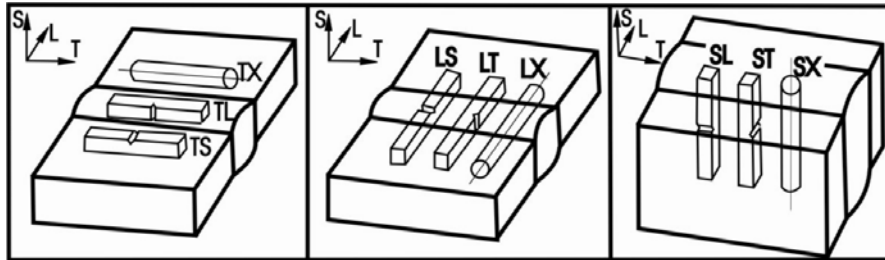


FIGURE 4.1 – Directions for positioning of Charpy and tensile specimens.

The impact Charpy were accomplished according to ASTM E 23 – 00 standard in specimen cooled in a cold liquid bath, to determine the curves of ductile-brittle transition for the underwater wet welding. Those curves were calculated using the tangent-hyperbolic equation.

The minimum impact absorbed energy was 3 J. The Charpy transition temperature curves for the submerged wet weld were accomplished at 0, 20, 40 and 60 wcm, as shown in FIG. 4.2 to 4.5, where the absorbed energies in impact in function of the temperature are presented. For each curve, points obtained experimentally in the impact Charpy testing in welded specimen in several temperatures were plotted.

In FIG. 4.2, transition curve for wet welded at 0 wcm is shown. The upper-shelf energy was superior to 46 J. The transition temperature equivalent to the absorbed energy of 28 J was approximately + 15 °C for welds at 0 wcm.

The impact tests were used to define the initial temperatures in order to evaluate the fracture toughness of all the materials with porosities. The tangent-hyperbolic curve was considered a good approach for obtaining a better correlation between the experimental data and the curve.

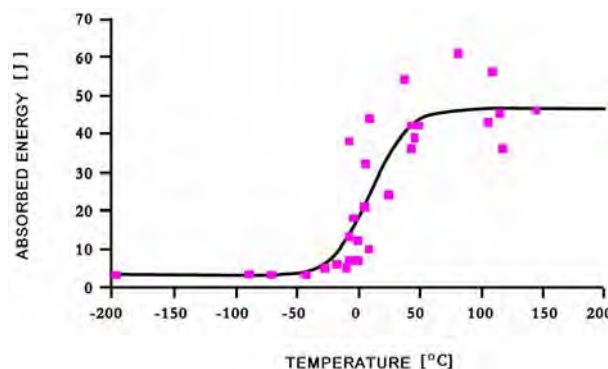


FIGURE 4.2 – Charpy transition temperatures curve for submerged wet welded at 0 wcm.

The Charpy impact transition temperature curve for underwater wet welded material at 20 wcm is shown in FIG. 4.3. The upper-shelf region of this weld is 41 J. The Charpy transition temperature at 28 J for the underwater wet welded material at 20 wcm was approximately + 5 °C. This indicated a decrease in the transition temperature of 10 °C between the material underwater wet welded at 20 wcm and 0 wcm. There was also a decrease in the energy in the upper-shelf in 5 J at the same depth.

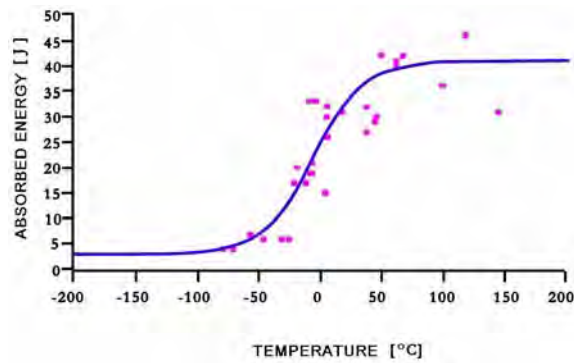


FIGURE 4.3 – Charpy transition temperature curve for underwater wet welded at 20 wcm.

The Charpy transition temperature curve for underwater wet welded at 40 wcm is shown in FIG. 4.4. The upper-shelf region of this weld is 33 J. The temperature of Charpy transition of 28 J for the underwater wet welded at 40 wcm was about - 5 °C.

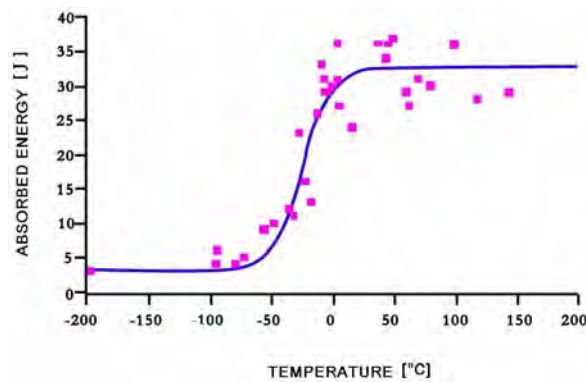


FIGURE 4.4 – Charpy transition temperature curve for underwater wet welded at 40 wcm.

The Charpy transition temperature curve for underwater wet welded material at 60 wcm is shown in FIG. 4.5. The upper shelf region of this weld is 31 J. The Charpy transition temperature of 28 J for the underwater wet welding to 60 wcm was about 20 °C.

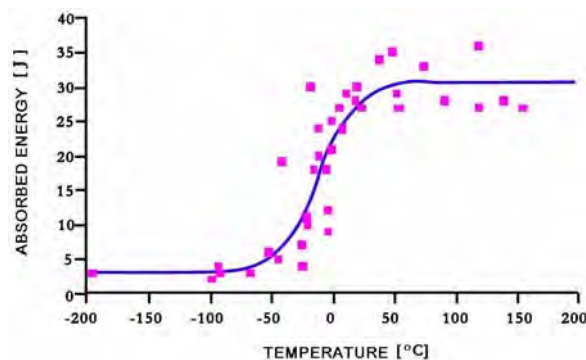


FIGURE 4.5 – Charpy transition temperature curve for underwater wet welded at 60 wcm.

The lateral expansion curve obtained in impact Charpy testing for the specimen welded in atmosphere underwater wet at 60 wcm is shown in FIG. 4.6. The lateral expansion in the upper-shelf region for this welding was about 0.71 mm.

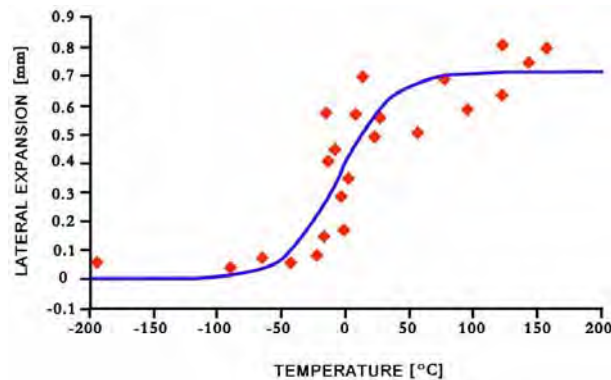


FIGURE 4.6 – Lateral expansion curve for impact on underwater wet welding at 60 wcm.

Four curves of transition of energy absorbed in the brittle-ductile range for underwater welded specimen at depths of 0, 20, 40 and 60 wcm are shown in FIG. 4.7. It can be observed that the transitions temperatures vary lightly with the absorbed energy, for instance, at 20 J or 28 J. Decreases of the maximum absorbed energies with the increase in the depth of underwater wet welding were also observed. It can also be observed in FIG. 4.7 that there is a decrease in the maximum absorbed impact energy with the increase of the depth of underwater wet welding, in the upper-shelf region, as proposed by Watson et alii (1994). However this was not significantly modified, according to the same author, but only between 0 wcm and 40 wcm. Reduction was smaller at 60 wcm. For underwater structures, the conventional use is higher than 0 °C in all the situations. In those cases the absorbed impact energies are, basically, in the upper-shelf region.

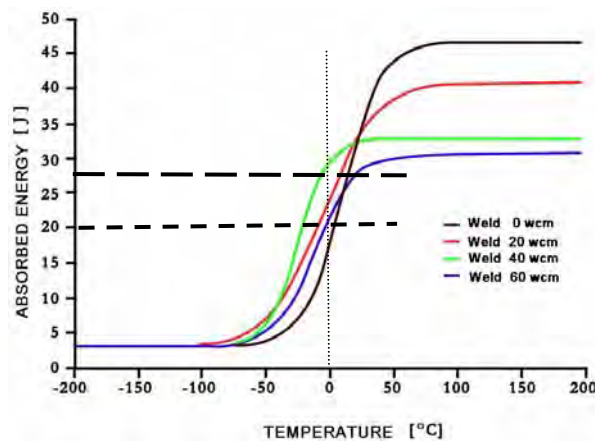


FIGURE 4.7 – Charpy transition temperature curve for underwater wet welding, performed at several depths. Curve using the approach of tangent-hyperbolic.

It was not possible to establish a well defined behavior for the changes in the Charpy transition temperatures for the steels welded in underwater wet condition at several depths for the absorbed energy and for the lateral expansion of the specimens. The magnitude order of temperature changes is the same, being the lowest transition temperature 40, 20, 60 and 0 wcm respectively, for an absorbed energy of 20 J. However, in the decreases of the maximum absorbed energy and in the maximum lateral expansion, in the region of the upper-shelf, the rules are very well established. The maximum absorbed energy as well as the maximum lateral expansion, happened in underwater wet welding at 0 wcm, but it was subsequently smaller for 20, 40 and 60 wcm.

The correlations between the absorbed energy for the theoretical Charpy transition temperature curve, calculated by the tangent-hyperbolic, and the experimental results obtained at each depth of underwater wet welding are shown in TAB. 4.1. The table also shows the correlations for lateral expansion of the welded samples.

In all experimental results, the impact Charpy testing in underwater wet welded specimens, the best correlation obtained was 40 wcm.

As can be observed in TAB. 4.1, the correlation between the experimental results and the tangent-hyperbolic theoretical curve for the absorbed energy indicates that approximately 90% of the samples tested at several depths

can be well represented by the proposed curves, with small exception for the underwater wet welding at 40 wcm, where the results were lightly better and reached 95%. A lightly best correlation was obtained for the lateral expansion properties of the samples.

TABLE 4.1 – Correlation between the Charpy impact results using Tangent-hyperbolic Curve for Transition Temperature Energy and Lateral Expansion.

Weld impact	Correlation for Absorbed Energy	Correlation for Lateral Expansion
Weld 0 wcm	88.2 %	94.4 %
Weld 20 wcm	88.6 %	90.8 %
Weld 40 wcm	95.1 %	91.6 %
Weld 60 wcm	89.3 %	89.6 %

The water temperatures vary with the sea depth. The depths can be: Surface (0 to 100 m), Central (100 to 500 m), Intermediate (500 to 1,000 m), Deep (1,000 to 3,000 m) and Under-deep (below 3,000 m). The medium temperatures of the water are: 27 °C for Surface water; 21 °C for Central; 7 °C for Intermediate; 4 °C for Deep and 2.8 °C for water of Under-deep, according to Santos (2000).

The present work is applied only to underwater wet welding at depths up to 60 wcm, in surface water, therefore with temperature higher then 20 °C.

Averages of the absorbed energies above 5 °C in impact Charpy specimen for underwater wet welded at several depths were calculated considering extreme situations.

Averages of absorbed energy for welds at 0, 20, 40 and 60 wcm are presented in FIG. 4.8. Limits of the confidence interval of 95% for the testing accomplished above +5 °C are also presented. A sigmoidal approach for the decrease in the absorbed energy exists for the average and for the confidence interval of 95%. The variation interval of energy for the welds at 0 wcm is larger than at 20, 40 and 60 wcm. This shows that in tests at larger depth, close to the upper-shelf of energy area, the interval has small variability.

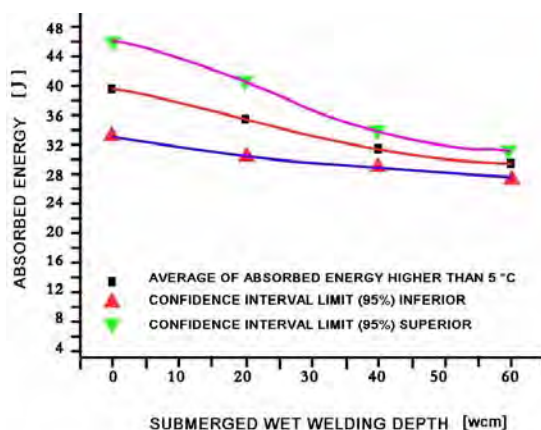


FIGURE 4.8 – Medium energy for impact Charpy testing performed at temperatures higher than 5 °C. (Confidence Interval of 95% for the experimental data).

The impact Charpy toughness in V notch reduces in a sigmoidal form, in agreement with the results obtained experimentally with the tested samples. This reduction tends, probably, to be asymptote for underwater wet welding at largest depths. According Watson et alii (1994), the impact Charpy toughness decreases with the increase in the welding depth. The same authors also state that the impact absorbed energy in the upper-shelf area decreases significantly with the increase in the depth of underwater wet welding. This does not agree in form with the results obtained in this work, where small decrease in the absorbed energy is observed in the upper-shelf region, when increases the welding depth between 40 and 60 wcm. The impact results obtained in this work agree basically with those described by Rowe and Liu (2001).

Total absorbed energy in the ductile transition curve for each welding depth was obtained by integrating the energy derivative. Points obtained by the integration of the absorbed energy curve derivative are shown in FIG. 4.9. A sigmoidal relationship of reduction of energy and welding depth is observed.

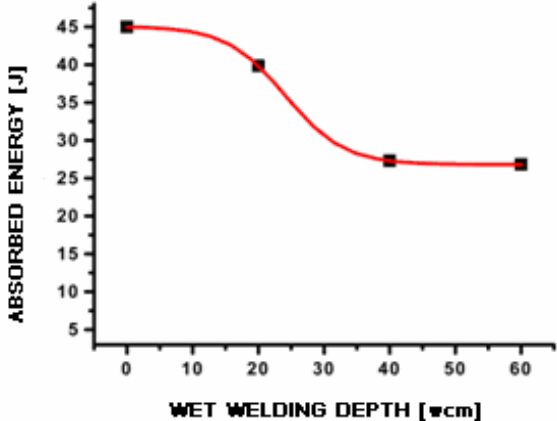


FIGURE 4.9 – Integral of the tangent-hyperbolic curve for the Charpy transition absorbed energy.

Similarly a sigmoidal relationship by the integration of the derived of the lateral expansion of underwater wet welded specimen at 0, 20, 40 and 60 wcm, as shown in FIG. 4.10, were also obtained.

Up to depth where the specimens were submitted to underwater wet welding and tested in impact Charpy, a decrease in the absorbed energy and in the lateral expansion with the increase of the depth was observed. The obtained behavior was sigmoidal in the tested region.

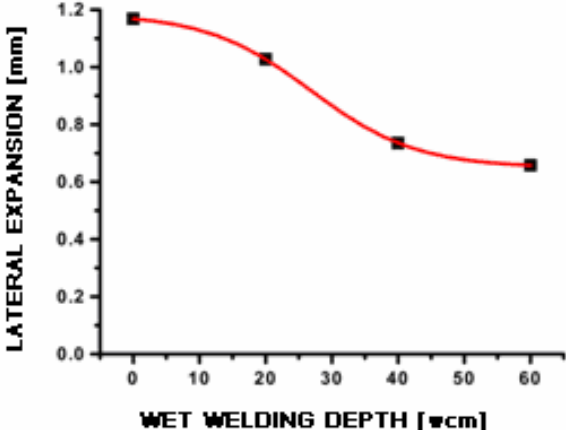


FIGURE 4.10 – Integral of the tangent-hyperbolic curve of transition for lateral expansion in function of the welding depth.

To evaluate the fracture toughness of the underwater wet welding, small size specimens were used. These specimen types for evaluating the fracture toughness are being developed to be used when are difficulties in producing larger samples, or conditioning them in special atmospheres, as in the case of nuclear power reactors, to estimate the future behavior after irradiation.

To characterize the fracture toughness of ferritic steels, typical of the underwater wet welding of this work, the reference temperature, T_0 , in which happened cleavage cracking in the elastic area or elastic-plastic instabilities, or both (ASTM E 1921 - 02) was determined.

According to ASTM E 1921 – 02 Standard the evaluation of the fracture toughness of no-uniform material doesn't answer to the statistical analysis used. The materials must have macroscopically uniform tensile and toughness properties.

In spite of the material produced by underwater wet welding have discontinuities type porosities, inherent to that process, it was considered as a uniform material in this work. The tensile properties and toughness were uniform. Another important point was that the fracture toughness in all tests was inside the tolerance limits (ASTM E 1921 - 02). Mechanical yield strengths were also practically inside the range 275 - 825 MPa.

To evaluate the fracture toughness of underwater wet welding at different depths samples was removed transversally from the center of welded plate. Those samples had a pre-crack opening done by fatigue equipment with the propagation direction similar to the one in the notch impact Charpy test. They were positioned in the L-T direction, as presented in FIG. 4.1.

The Charpy impact temperatures for 28 J, determined in Charpy transition curve for all underwater wet welding, were +15 °C at 0 wcm; 5 °C at 20 wcm; - 5 °C at 40 wcm and 20 °C at 60 wcm, and served as base for beginning the testing of fracture toughness increasing - 50 °C to the equivalent temperature for 28 J. The testing of fracture toughness performed at the temperatures of - 35 °C, - 45 °C, - 55 °C, - 35 °C for underwater wet welding at respectively 0, 20, 40 and 60 wcm, showed to be totally ductile; without any brittle growth, and, therefore, impossible to be used for determining the reference temperatures, T_0 . The reference temperature is determined for fractures by cleavage in the region of elastic instability or elastic-plastic instabilities.

All tests for fracture toughness of underwater wet welding at different depths were performed, starting from the previous results, in multi-temperatures, but close to - 100 °C. In these temperatures cleavage or at least minimum fracture instability in specimens tested were observed.

The Weibull model was used to obtain the reference temperature T_0 and the stress intensity factor equivalent to the elastic-plastic K_{Jc} derived from the Integral-J in the point at the beginning of the cleavage fracture, J_c .

From the dimensions of the specimen, the testing temperature and the mechanical force on the sample K_0 , K_{Jc} , T_0 , and the limits of tolerance were determined. (K_0 is the scale parameter of the Weibull curve; K_{Jc} is the stress intensity factor calculated from the J-integral; T_0 is the reference temperature in which the median of the distribution of K_{Jc} for the samples of size 1T (25.4 mm) it is same to 100 MPa).

Results of stress intensity factor corrected by sample 1T with the temperatures of testing for underwater wet welding at different depths are shown in FIG 4.11 to 4.14. In these Master Curve figures, the limits with 95% of superior tolerance and 5% in the inferior are plotted.

In all situations of underwater wet welding the samples were tested to obtain at least 9 valid data of K_{Jc} .

In the censored values of fracture toughness the values of K_{Jc} are substituted by calculated $K_{Jc(limit)}$. In the calculation of the reference temperature T_0 for multi-temperatures test, as considered in the present work, coefficients is 1 for valid values, and equal to 0 for the dummy values, in other words, the censored values.

The samples for fracture toughness test of all underwater wet welded at different depths were conditioned to test at temperature in a dry refrigeration chamber, during at least 15 minutes before the tests.

In FIG. 4.11 Master Curves for the underwater wet welded at 0 wcm are shown. Those curves were calculated from 9 valid tests and 1 censored value, and the following results were obtained:

$$K_0 = 81.1 \text{ MPa}$$

$$K_{Jc (median)} = 75.7 \text{ MPa}$$

$$T_0 = - 90 \text{ }^\circ\text{C}$$

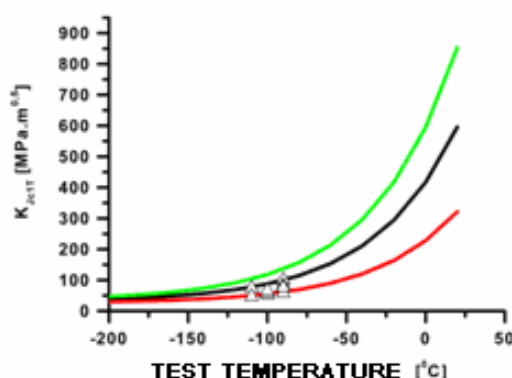


FIGURE 4.11 – Master curve for underwater wet welding at 0 wcm, with limits of tolerance superior equal to 95% and inferior equal to 5%.

The valid tests and the censored value of fracture toughness for the underwater wet welding at 0 wcm were performed in the temperatures range - 90 to - 110 °C. The tests in higher temperatures, - 50 to - 70 °C, close to the

ones suggested by ASTM E 1921 – 02 standard, from the impact results Charpy, were discarded because they were considered no-test (samples without any cleavage fracture).

Master Curves for the underwater wet welded at 20 wcm are shown in FIG. 4.12. These curves were calculated from 14 valid tests and 3 censored value, and the following results were obtained:

- $K_0 = 65.7 \text{ MPa}$
- $K_{Jc(\text{median})} = 61.7 \text{ MPa}$
- $T_0 = - 84 \text{ }^\circ\text{C}$

The valid results and the censored values for fracture toughness in underwater wet welded at 20 wcm were performed in the temperatures range - 90 to - 115 $^\circ\text{C}$. The tests at higher temperatures, of the order of - 50 $^\circ\text{C}$, close to the value suggested by ASTM E 1921 - 02 from the Charpy impact results, were discarded because no-test were considered (samples without any cleavage fracture).

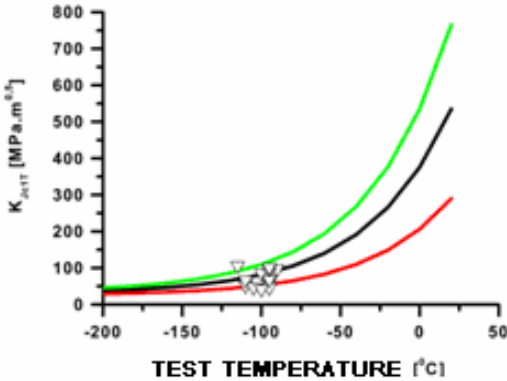


FIGURE 4.12 – Master curves for underwater wet welding at 20 wcm with limits of tolerance superior equal to 95% and inferior equal to 5%.

Curves for the underwater wet welded at 40 wcm are shown in FIG. 4.13. These curves were calculated from 9 valid tests, more 1 censored value, and the following results were obtained:

- $K_0 = 80.9 \text{ MPa}$
- $K_{Jc(\text{median})} = 75.5 \text{ MPa}$
- $T_0 = - 80 \text{ }^\circ\text{C}$

The valid test and the censored value of fracture toughness for the underwater wet welded at 40 wcm were accomplished in the temperatures range - 95 to - 110 $^\circ\text{C}$. Specimens tested at temperatures of an order of - 50 $^\circ\text{C}$ were discharged, close to the suggested by ASTM E 1921 - 02 from the Charpy impact results, because no-test was considered (samples without any cleavage fracture).

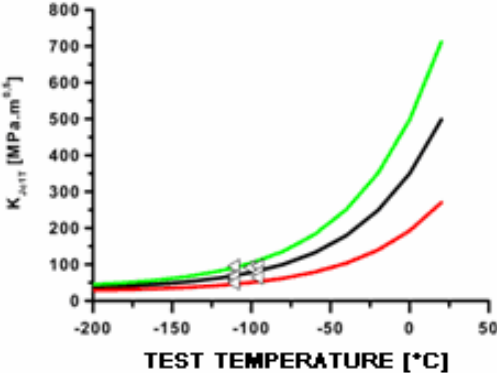


FIGURE 4.13 – Master curves for underwater wet welding at 40 wcm, with limits of tolerance superior of 95% and inferior of 5%.

Master Curves for the underwater wet welded at 60 wcm are shown in FIG. 4.14. These curves were calculated from 12 valid more 3 censored tests, and the following results were obtained:

$$K_0 = 79.5 \text{ MPa}$$

$$K_{Jc \text{ (median)}} = 74.3 \text{ MPa}$$

$$T_0 = -78 \text{ }^\circ\text{C}$$

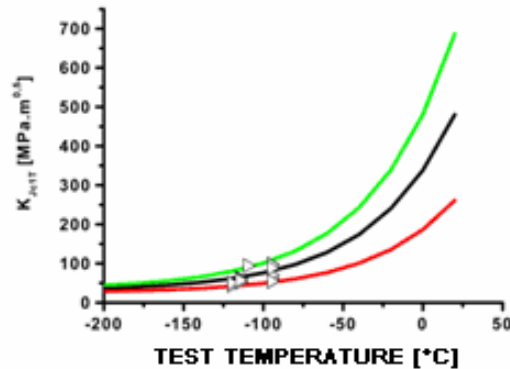


FIGURE 4.14 – Master curves for underwater wet welding at 60 wcm, with limits of tolerance superior of 95% and inferior of 5%.

The valid and censored results from the fracture toughness of underwater wet welded at 60 wcm were accomplished in the temperatures range - 90 to - 120 °C. Tests at higher temperatures of - 50 °C, close to the one suggested by the ASTM E 1921 - 02 from the impact results Charpy, were discarded because no-test were considered no-test (samples without any cleavage fracture).

The references temperatures obtained for underwater wet welded materials at 0, 20, 40 and 60 wcm were growing, using the method proposed by ASTM E 1921 - 02. There were obtained at temperatures - 90; - 84; - 80 and - 78 °C, respectively.

Submerged structures working in temperatures higher then those at corresponding to the reference temperatures have a ductile behavior. Results observed by Dexter et alii (1986), as larger the depth of underwater wet welding smaller the toughness, supported by the increase of the reference temperatures were confirmed.

Inside the temperature range tested in fracture toughness of underwater wet welding, instability plastic and any ductile growth of crack were not observed.

In spite of the structures produced by underwater wet welding have high discontinuities levels, frequently they are used in submerged environment. This is the principal reason to work with underwater wet welded fracture toughness, contradicting the results of Kober et alii (1995)- fracture mechanics it is not usually applied in such conditions.

The variability of the fracture toughness tests was lightly wide in the lower-shelf area, for the determining the reference temperature. However, these variability were inside the values specified by ASTM E 1921 - 02. It was not tested with any fibrous crack, since even the pre-cracking-of fatigue was always in the cleavage area.

In general, when increasing the depth of underwater wet welding the limits of tensile resistance decrease; superficial porosities of the welds bead increases; the hardness Vickers of the welds bead decrease; increase the porosities in solidification directions; increases the reference temperature of the fracture toughness.

For larger porosities densities, in underwater wet welding at higher depths, smaller are the absorbed energies in Charpy impact. The same happens with the fracture toughness that has an increase in the reference temperature with the increase in the depth of underwater wet welding.

Tests of fracture toughness according to the ASTM E 1921 - 02 demand a minimum number of samples, usually 6 - 8 from the valid data. With these small numbers of specimens, used in this work, other statistical distributions, different from Weibull, were tested. The distributions tested were: normal, log-normal and Weibull with the obtained experimental data of fracture toughness of underwater wet welding at different depths. The correlation coefficients linear and Anderson-Darling statistic for the experimental data of the fracture toughness of the underwater wet welding at different depths were computed, and are presented in TAB. 4.2. Obtained results suggested that the distribution of Weibull is not the best one to be used for the experimental data of this work.

Statistical evaluations of fracture toughness should be done for a better proof of the distribution type that would be more acceptable to be used in the underwater wet welding.

From the results of this work it is important to observe that although the levels of energies absorbed in Charpy transition temperatures curve are relatively low, the Charpy transition temperatures for other structural materials

are lower. This is also verified in relation to the fracture toughness where were obtained temperatures of references T_0 below -75°C indicating that the material has good fracture toughness.

It can be observed in TAB. 4.2 that the correlation as well as the coefficient of Anderson-Darling obtained in the underwater wet welding at 60 wcm is very different from the one at other depths. This could be justified because the underwater wet weld material at 60 wcm has resistance properties very close to the inferior limit of ASTM E 1921 – 02 standard acceptable values.

TABLE 4.2 – Coefficients of Correlation Linear and of Anderson-Darling Statistic for the experimental data obtained in the fracture toughness tests.

Underwater Wet Welding	Statistical Distribution	Correlation Coefficient	Anderson-Darling
0 wcm	Weibull	96.8 %	3.516
	Lognormal	99.1 %	3.134
	Normal	97.5 %	3.249
20 wcm	Weibull	93.7 %	6.153
	Lognormal	97.2 %	5.251
	Normal	94.8 %	5.520
40 wcm	Weibull	96.8 %	3.427
	Lognormal	98.6 %	3.130
	Normal	97.3 %	3.218
60 wcm	Weibull	86.5 %	17.900
	Lognormal	90.7 %	15.589
	Normal	85.0 %	16.009

5. CONCLUSIONS

Conclusions concerning to the mechanical behavior of the underwater wet weld are:

1. Toughness of underwater wet welding varies with weld depth.
2. A dispersion of the results of impact of the underwater wet welding for determining the Charpy transition temperature curve occurs.
3. In the underwater wet welding of this work a very established the upper-shelf areas in impact was observed. As smaller the depth of underwater wet welding, higher are the energy absorbed in impact.
4. In the region of ductile-fragile transition, between upper and lower-shelf, the behavior in impact diverges. There are inversions of results between 20 and 28 J.
5. There is a strong linear correlation between the absorbed energy and the lateral expansion in Charpy impact tests for the underwater wet welding samples.
6. Toughness of impact Charpy decrease sigmoidal with the depth in temperatures higher then 5°C .
7. Specimens submitted to underwater wet welding behaves as uniform materials in the fracture toughness.
8. Charpy transition temperature is not a good indication for determining the reference temperature in fracture toughness tests, as suggested by ASTM E 1921 - 02.
9. The Weibull model, proposed by ASTM E 1921 - 02, is not the best for determining the reference temperature in fracture toughness.
10. The reference temperatures in fracture toughness increase when underwater wet welding depth increases. .
11. In conventional operation temperatures of submerged structures, underwater wet welding presented ductile behavior.

Structures built using underwater wet welding up to 60 wcm that work inside water in conventional temperatures, behave as "ductile", in spite of the great number of present discontinuities in these weld.

REFERENCES

- AMERICAN SOCIETY FOR TESTING AND MATERIALS. **ASTM E 23 - 00** – “Notched Bar Impact Testing of Metallic Materials”, Vol. 3.01 – Annual Book of ASTM Standards 2001.
- AMERICAN SOCIETY FOR TESTING AND MATERIALS. **ASTM E 1921 - 02** – “Standard Test Methods for Determination of Reference Temperature, T_0 , for Ferritic Steels in the Transition Range” – American Society for Testing Materials, 2002.
- AMERICAN WELDING SOCIETY. **AWS D 3.6 - 99** – “Specification for Underwater Welding” – American Welding Society - 1999.
- DANNINGER, H.; JANGG, G.; WEISS, B.; STICKLER, R. **Microstructure and Mechanical Properties of Sintered Iron**. Part II: Experimental Study - Powder Metallurgy International, Vol. 25. n0 4 - pp. 170-173 - 1993.
- DI LORENZO, R.F.; ALENCAR, D.A.; SILVA, W.A.; BRACARENSE, A.Q.; LIU, S. **Stability of Shielded Metal Arc Welding Transfer in Wet Under-Fresh-Water Welding**. Proceeding OMAE2001-3231: 20th International Conference on *Offshore* Mechanics and Arctic Engineering, June 3-8, 2001, Rio de Janeiro, Brasil.
- IBARRA, S.; OLSON, D. L. **Underwater Welding of Steel**. Engineering Materials, Vol. 69 & 70 – 1992 – pp. 329-378.
- KOBER, G.R.; DEXTER, R.J.; KAUFMANN, E.J.; YEN, B.T.; FISCHER, J.W. **The Effect of Welding Discontinuities on the Variability of Fatigue Life**. Fracture Mechanics: 25th Volume, ASTM STP 1220, F. Erdogan, Ed., American Society for Testing and Materials, Philadelphia, 1995.
- KOÇAK, M.; SCHWALBE, K.H. **Fracture Mechanics of Weldments: Microstructural, Experimental and Mechanical Aspects**. Proceedings of Ninth European Conference of Fracture – Vol. II – Varna, Bulgaria, Sept. 21-25, 1992.
- LIU, S.; POPE, A.M.; DAEMEN, R. **Welding Consumable and Weldability** - INTERNATIONAL WORKSHOP ON UNDERWATER WELDING OF MARINE STRUCTURES - December 7-9, 1994, New Orleans, Louisiana, USA, AMERICAN BUREAU OF SHIPPING.
- MATLOCK, D.K.; EDWARDS, G.R.; OLSON, D.L.; IBARRA, S. **Effect of Sear Water on Fatigue Crack Propagation Characteristics of Welds for Offshore Structures**. Journal Materials Engineering, Vol. 9 – No. 1 – pp. 25-34 – 1987.
- NEVASMAA, P.; BANNISTER, A.; WALLIN, K. **Fracture Toughness Estimation Methodology in the ‘SINTAP’ Procedures**. 17th International Conference on *Offshore* Mechanics and Arctic Engineering by ASME – OMAE98-2053, 1998.
- POPE, A.M.; MEDEIROS, R.C.; LIU, S. **Solidification of underwater wet welds**. 1995 OMAE – Vol. III, Material Engineering - ASME 1995.
- ROWE, M.; LIU, S. **Recent developments in underwater wet welding**. Science and Technology of Welding and Joining, Vol. 6 N.6 – pp. 387-396 – 2001.
- SANTOS, F. A. **Relação entre a Profundidade de Topo da Água Central do Atlântico Sul e a Concentração de Clorofila na Coluna D’água**. MCT, Instituto Nacional de Pesquisas Espaciais, INPE – Julho 2000.
- SUGA, Y.; HASUI, A. **On Formation of Porosity in Underwater Weld Metal**. Transaction JWS, Vol. 17, N° 1 - April 1986 - Doc IX 1388-86.
- WATSON, P.D.; TSAI, C.L.; WOOD, B. **Fitness of service design application for underwater wet welds**. INTERNATIONAL WORKSHOP ON UNDERWATER WELDING OF MARINE STRUCTURES - December 7-9, 1994, New Orleans, Louisiana, USA, AMERICAN BUREAU OF SHIPPING. page 201-236.
- WELDING HANDBOOK - **Materials and applications** - Part 1 - Eighth Ed. American Welding Society, 1996.